

The University of Bradford Institutional Repository

<http://bradscholars.brad.ac.uk>

This work is made available online in accordance with publisher policies. Please refer to the repository record for this item and our Policy Document available from the repository home page for further information.

To see the final version of this work please visit the publisher's website. Access to the published online version may require a subscription.

Link to publisher's version: <http://dx.doi.org/10.1016/j.cej.2016.12.096>

Citation: Al-Obaidi MA, Li J-P, Kara-Zaitri C et al (2017) Optimisation of reverse osmosis based wastewater treatment system for the removal of chlorophenol using genetic algorithms. Chemical Engineering Journal. 316: 91-100.

Copyright statement: © 2017 Elsevier B.V. Reproduced in accordance with the publisher's self-archiving policy. This manuscript version is made available under the [CC-BY-NC-ND 4.0](https://creativecommons.org/licenses/by-nc-nd/4.0/) license.



Optimisation of reverse osmosis based wastewater treatment system for the removal of chlorophenol using Genetic Algorithms

M. A. Al-Obaidi ^{1,2}, J-P Li ¹, C. Kara-Zaitri ¹ and I. M. Mujtaba ^{1,*}

¹ Chemical Engineering Division, School of Engineering, University of Bradford,
Bradford, West Yorkshire BD7 1DP, UK

² Middle Technical University, Iraq – Baghdad

*Corresponding author, Tel.: +44 0 1274 233645

E-mail address: I.M.Mujtaba@bradford.ac.uk

Abstract

Reverse Osmosis (RO) has found extensive applications in industry as an efficient separation process in comparison with thermal process. In this study, a one-dimensional distributed model based on a wastewater treatment spiral-wound RO system is developed to simulate the transport phenomena of solute and water through the membrane and describe the variation of operating parameters along the x-axis of membrane. The distributed model is tested against experimental data available in the literature derived from a chlorophenol rejection system implemented on a pilot-scale cross-flow RO filtration system with an individual spiral-wound membrane at different operating conditions. The proposed model is then used to carry out an optimisation study using a Genetic Algorithm (GA). The GA is developed to solve a formulated optimisation problem involving two objective functions of RO wastewater system performance. The model code is written in MATLAB, and the optimisation problem is solved using an optimisation platform written in C++. The objective function is to maximize the solute rejection at different cases of feed concentration and minimize the operating pressure to improve economic aspects. The operating feed flow rate, pressure and temperature are considered as decision variables. The optimisation problem is subjected to a number of upper and lower limits of decision variables, as recommended by the module's manufacturer, and the constraint of the pressure loss along the membrane length to be within the allowable

value. The algorithm developed has yielded a low optimisation execution time and resulted in improved unit performance based on a set of optimal operating conditions.

Keywords: Spiral-wound reverse osmosis; Wastewater treatment; One-dimensional modelling;

Optimisation; Genetic algorithm.

1. Introduction

The use of Reverse Osmosis (RO) is becoming more and more popular in seawater and wastewater treatment because of the low cost of water production and solute rejection compared to other thermal processes [1]. A number of studies have been conducted to maximize the performance of the system. Such studies have investigated the transport phenomena of water and solute through the membrane by improving current mathematical models and identifying the optimum set of operating variables. The optimisation of seawater RO desalination system has been carried out using different methods including, global optimisation algorithm [1], Sequential Quadratic Programming (SQP) [2], Mixed-Integer Non-Linear Programming (MINLP) [3], Genetic Algorithm (GA) [4] and multi-objective optimisation and genetic algorithm (MOO+GA) [5]. In many applications, the use of GA has yielded better results in optimisation in comparison to other conventional methods [6]. For instance, GAs have been used extensively in different areas of chemical engineering process design and operation, such as, distillation system [7], semi-batch reactor [8], multi-phase catalytic reactor (hydrogenation reaction system) [9], microchannel reactor (emerged as a novel technology for the synthesis of liquid hydrocarbons applications) [10] and steam reforming of hydrocarbons for the generation of hydrogen and synthesis gas [11]. Also, [Fang et al.](#) [12] have combined an integrated Neural Network (NN) dynamic model and GA

approach to optimise the performance of a full-scale municipal wastewater treatment plant with substantial influent fluctuations.

The use of GA to optimise the seawater RO desalination processes has already been implemented in a number of studies. [Guria et al. \[5\]](#) used the multi-objective optimisation and Non-dominated Sorting Genetic Algorithm (NSGA) technique for desalination of seawater using a spiral-wound and tubular RO modules. The optimisation problem consisted two or three objective functions of maximizing the water flux in addition to minimizing the permeate concentration and cost of filtration of a real existing plant. [Murthy and Vengal \[4\]](#) used a single objective genetic algorithm technique (SGA) to optimize the rejection of NaCl in a laboratory scale RO desalination system of a disc-shaped flat cellulose acetate membrane. The experiments were carried out by varying the inlet feed flow rate and the overall water flux at constant feed concentration. In this study, the mechanism of water and solute transport are measured using the Spiegler and Kedem model. [Djebedjian et al. \[13\]](#) implemented GA with a solution-diffusion model to optimize the performance of a real RO desalination plant predicted the best operating pressure difference across the membrane, which enhances the water flux with low permeate concentration. Moreover, the modelling and prediction of the membrane fouling rate in a micro-filtration (MF) pilot-scale drinking water production system was achieved using the genetic programming by [Lee et al. \[14\]](#). [Park et al. \[15\]](#) used GA for analysing the performance of pilot-scale RO system. Finally, [Bourouni et al. \[16\]](#) used GA to optimise the optimal configuration of a hybrid system of a small RO unit coupled with renewable energy source (photovoltaic and wind).

In contrast, to the best of our knowledge, the optimisation of RO based wastewater treatment using GA has been rarely used to find the optimal values of operation that can be achieved within the manufacturer specification. [Okhovat and Mousavi \[18\]](#) used GA to model the rejection of arsenic, chromium and cadmium ions as a function of transmembrane pressure

and initial concentration of pollutants in a nanofiltration (NF) pilot-scale system. [Soleimani et al. \[19\]](#) investigated the treatment of oily wastewaters with commercially polyacrylonitrile (PAN) ultra-filtration (UF) membranes by using artificial neural networks (ANNs) to predict the permeation flux and fouling resistance. GA was then used to optimize the operating conditions of trans-membrane pressure, cross-flow velocity, feed temperature and pH. The objective was to maximize the permeation flux while minimizing the fouling behaviour.

To the best of author's knowledge, there has not been any study that uses GA optimisation technique for distributed model for optimising the removal of organic compound such as chlorophenol using a spiral-wound RO process. Therefore, this paper aims to present a one-dimensional model for the rejection of chlorophenol from aqueous solution of different concentrations using a pilot-scale of an individual TFC Polyamide spiral-wound RO filtration system. The distributed model is able to give an accurate picture of the transport across the membrane. An optimisation study of chlorophenol rejection is subsequently implemented using GA. The optimisation process is carried out by manipulating the inlet decision variables of the feed pressure, flowrate and temperature for five different feed concentrations of chlorophenol. The optimized rejections with a constraint of low pressure loss were investigated to provide further evidence of the results.

2. Modelling and simulation of spiral-wound RO

The main objective of this section is to develop a one-dimensional distributed model that can be used to predict accurately the variation of operating parameters along the x-axis of membrane. It is important to understand the interaction between the transport theories through the membrane in order to develop a numerical model that incorporates the spatial variation in fluid properties.

2.1 Assumptions

The following assumptions are made to develop the proposed process model:

1. The solution-diffusion model is used for mass transport through the module.
2. The membrane characteristics and the channel geometries are assumed constant.
3. Validity of Darcy's law where the friction parameter is used to characterize the pressure drop in the feed channel.
4. Constant atmospheric pressure at the permeate channel.
5. A constant solute concentration is assumed in the permeate channel and the average value will be calculated from the inlet and outlet permeate solute concentrations.
6. The underlying process is assumed to be isothermal.

2.2 Governing equations

The water $J_{w(x)}$ and solute $J_{s(x)}$ fluxes (m/s, kmol/m² s) can be calculated using the solution-diffusion model of [Lonsdale et al. \[20\]](#) (Assumption 1):

$$J_{w(x)} = A_w (\Delta P_{b(x)} - \Delta \pi_{s(x)}) \quad (1)$$

$$J_{s(x)} = B_s (C_{w(x)} - C_{p(av)})$$

(2)

Where A_w , B_s , $\Delta P_{b(x)}$ and $\Delta \pi_{s(x)}$ are solvent transport coefficient (m/atm s), solute permeability coefficients of the membrane (m/s), pressure difference and osmotic pressure difference at any point along the x-axis (atm) respectively. Also, $C_{w(x)}$ and $C_{p(av)}$ (kmol/m³) are the molar solute concentration on the membrane surface and the average permeate concentration respectively.

The pressure difference between the feed and permeate channels at any point, $\Delta P_{b(x)}$ (atm), is related to the pressure in both the feed and permeate channels.

$$\Delta P_{b(x)} = P_{b(x)} - P_p \quad (3)$$

Where $P_{b(x)}$ and P_p (atm) are the feed at any point along the feed channel and constant permeate pressure ([Assumption 4](#)) respectively.

The following two equations work well for solute flux and the difference of osmotic pressure:

$$J_{s(x)} = J_{w(x)} C_{p(av)} \quad (4)$$

$$\Delta \pi_{s(x)} = R T_b (C_{w(x)} - C_{p(av)})$$

(5)

$$\Delta \pi_{s(x)} = R T_b \left(\frac{J_{s(x)}}{B_s} \right) \quad (6)$$

Where R and T_b ($\frac{\text{atm m}^3}{\text{K kmol}}$ and K) are the gas constant and constant brine temperature ([Assumption 6](#)) respectively. The combination of [Eqs. \(4\), \(6\)](#) and [\(1\)](#) gives.

$$J_{w(x)} = A_w \left(\Delta P_{b(x)} - R T_b \frac{J_{w(x)} C_{p(av)}}{B_s} \right)$$

(7) Re-arranging of [Eq. \(7\)](#) yields.

$$J_{w(x)} = \frac{A_w B_s \Delta P_{b(x)}}{B_s + R T_b A_w C_{p(av)}} \quad (8)$$

[Eq. \(8\)](#) can be simplified to:

$$J_{w(x)} = \theta \Delta P_{b(x)} \quad (9)$$

Where

$$\theta = \frac{A_w B_s}{B_s + R T_b A_w C_{p(av)}}$$

(10)

Specifically, the total mass balance and solute balance in both channels can be written as:

$$F_{b(0)} = F_{b(x)} + F_{p(x)}$$

(11)

$$F_{b(0)}C_{b(0)} = F_{b(x)}C_{b(x)} + F_{p(x)}C_{p(av)}$$

(12)

$F_{b(0)}$, $F_{b(x)}$, $F_{p(x)}$ (m^3/s), $C_{b(0)}$ and $C_{b(x)}$ ($kmol/m^3$) are feed flow rate at the entrance and at any point in the feed channel, permeate flow rate, feed concentration at the entrance and at any point along the x-axis respectively. Also, Darcy's law can be used to describe the drop of pressure in both channels in the feed channel ([Assumption 3](#)).

$$\frac{dP_{b(x)}}{dx} = -b F_{b(x)}$$

(13)

Where b ($atm\ s/m^4$) is the feed channel friction parameter.

While, the derivation of [Eq. \(11\)](#) with the x-axis, gives:

$$\frac{dF_{b(x)}}{dx} = -\frac{dF_{p(x)}}{dx} = -W J_{w(x)}$$

(14)

Where, W (m) is the width of membrane. Dividing [Eqs. \(13\)](#) and [\(14\)](#) gives:

$$\frac{dP_{b(x)}}{dF_{b(x)}} = \frac{b F_{b(x)}}{W J_{w(x)}}$$

(15)

Finally, the re-arrangement and integration of [Eq. \(15\)](#) yields the specific equations of the model used for simulation as follows:

The feed flow rate $F_{b(x)}$ (m³/s) at any point along the x-axis is calculated as:

$$F_{b(x)} = \left\{ F_{b(0)} - (W \theta x \Delta P_{b(0)}) + \left(W \theta b \left(\frac{x^2}{2} \right) F_{b(0)} \right) + \left(W \theta b \left(\frac{W \theta}{b} \right)^{0.5} \left(\frac{x^2}{2} \right) (\Delta P_{b(x)} - \Delta P_{b(0)}) \right) \right\} \quad (16)$$

Where x is the coordinate of the x-axis under consideration. The feed pressure $P_{b(x)}$ (atm) and pressure difference $\Delta P_{b(x)}$ (atm) at any point along the x-axis are calculated by [Eqs. \(17\)](#) and [\(18\)](#):

$$P_{b(x)} = \left\{ P_{b(0)} - (b x F_{b(0)}) + \left(b W \theta \left(\frac{x^2}{2} \right) (\Delta P_{b(x)}) \right) - \left[b^2 W \theta \left(\frac{x^3}{6} \right) F_{b(0)} \right] - \left[b^2 W \theta \left(\frac{W \theta}{b} \right)^{0.5} \left(\frac{x^3}{6} \right) (\Delta P_{b(x)} - \Delta P_{b(0)}) \right] \right\} \quad (17)$$

$$\Delta P_{b(x)} = \Delta P_{b(0)} - (b x F_{b(0)}) - \left[\left(\frac{W \theta}{b} \right)^{0.5} b x (\Delta P_{b(x)} - \Delta P_{b(0)}) \right] \quad (18)$$

The pressure loss (atm) along the membrane length is calculated using [Eq. \(19\)](#).

$$P_{loss} = P_{b(0)} - P_{b(L)} \quad (19)$$

The water flux $J_{w(x)}$ (m/sec) depicts in the counter of [Eq. \(20\)](#).

$$J_{w(x)} = \theta \left\{ [\Delta P_{b(0)} - (b x F_{b(0)})] - \left[\left(\frac{W \theta}{b} \right)^{0.5} b x (\Delta P_{b(x)} - \Delta P_{b(0)}) \right] \right\} \quad (20)$$

Eq. (20) illustrates that increasing applied pressure $\Delta P_{b(0)}$ would increase the water flux through the membrane. Also, it is usual expectation that increasing inlet feed concentration would increase the diffusivity, density and viscosity parameters (Appendix A), which reduces the flux of water. However, this would also increase the concentration polarization impact that causes an increase in wall membrane concentration and increases of osmotic pressure. More often than not, increasing inlet feed temperature will decrease the viscosity and density parameters and increases the diffusivity parameter that increases the mass transfer coefficient and lifts up the water flux.

Eq. (21) is used to calculate the feed concentration $C_{b(x)}$ (kmol/m³) along the x-axis.

$$C_{b(x)} = \frac{F_{b(x-1)}(C_{b(x-1)} - C_{p(av)})}{F_{b(x)}} + C_{p(av)} \quad (21)$$

While the permeate solute concentration $C_{p(av)}$ (kmol/m³) is calculated using Eq. (22) by taking the average of the inlet and outlet permeate concentrations $C_{p(0)}$ and outlet $C_{p(L)}$ (kmol/m³) as can be shown in Eqs. (23) and (24) (Assumption 5) [21].

$$C_{p(av)} = \frac{C_{p(0)} + C_{p(L)}}{2} \quad (22)$$

$$C_{p(0)} = \frac{B_s C_{b(0)} e^{\frac{J_{w(0)}}{k(0)}}}{J_{w(0)} + B_s e^{\frac{J_{w(0)}}{k(0)}}} \quad (23)$$

$$C_{p(L)} = \frac{B_s C_{b(L)} e^{\frac{J_{w(L)}}{k(L)}}}{J_{w(L)} + B_s e^{\frac{J_{w(L)}}{k(L)}}} \quad (24)$$

Then, the permeate flow rate $F_{p(x)}$ (m³/s) is calculated by:

$$F_{p(x,y)} = F_{p(0)} + (W x \theta \Delta P_{b(0)}) - \left[W \theta b \left(\frac{x^2}{2} \right) F_{b(0)} \right] -$$

$$\left[W \theta b \left(\frac{x^2}{2} \right) \left(\frac{W \theta}{b} \right)^{0.5} (\Delta P_{b(x)} - \Delta P_{b(0)}) \right]$$

(25)

The mass transfer coefficient $k_{(x)}$ (m/s) is a function of pressure, concentration, flow rate and temperature, which means that it will vary with the membrane length. $k_{(x)}$ along the feed channel side has been found experimentally and calculated from Eq. (26) [22] as follows:

$$k_{(x)} d e_b = 147.4 D_{b(x)} Re_{b(x)}^{0.13} Re_{p(x)}^{0.739} C_{m(x)}^{0.135}$$

(26)

C_m is a dimensionless solute concentration and can be calculated by.

$$C_{m(x)} = \frac{C_{b(x)}}{\rho_w}$$

(27)

Where, ρ_w is the molal density of water (55.56 kmol/m³).

The feed velocity $U_{b(x)}$ (m/s) is calculated using Eq. (28).

$$U_{b(x)} = \frac{F_{b(x)}}{t_f W}$$

(28)

The concentration at the wall membrane $C_{w(x)}$ (kmol/m³) is calculated using Eq. (29).

$$\frac{C_{w(x)} - C_{p(av)}}{C_{b(x)} - C_{p(av)}} = \exp\left(\frac{J_{w(x)}}{k_{(x)}}\right)$$

(29)

Finally, Eqs (30) and (31) are used to calculate the solute rejection (dimensionless) [22] and total water recovery (dimensionless).

$$Rej = \frac{C_{b(L)} - C_{p(av)}}{C_{b(L)}} \times 100$$

(30)

$$Rec = \frac{F_{p(L)}}{F_{b(0)}} \times 100$$

(31)

The model equations presented have been solved within MATLAB, where the filtration channel is divided into a number of segments of equal intervals (Δx). For a given inlet feed flow rate, pressure, solute concentration and temperature, the proposed model can be used to predict the longitudinal variation of all parameters in the feed and permeate channels in the x-axis by using the estimated values of membrane transport parameters.

2.3 The physical properties equations

This study covers the experimental work of dilute chlorophenol aqueous solutions on spiral-wound module, so the physical properties equations of the solution has been conceived as identical to water equations proposed by [Koroneos \[23\]](#). The set of physical properties equations is presented in Appendix A.

3. Validation of the developed RO model

3.1 Experimental apparatus and procedure

A pilot-scale experiment has been set and consists of a cross-flow RO filtration system of one commercial thin film composite RO membrane packed into a spiral-wound module of

aqueous feed solutions of chlorophenol of specific concentration. The module was from the Ion Exchange Ltd. Company of India and used by Sundaramoorthy et al. [22]. The characteristics of the spiral-wound module and the transport parameters of this model (A_w , B_s and b) were given in Table 1. The feed was pumped in three different flow rates of $2.166\text{E-}4$, $2.33\text{E-}4$ and $2.583\text{E-}4$ m^3/s . Also, for each feed flow rate, the solute concentrations vary from $0.778\text{E-}3$ to $6.226\text{E-}3$ kmol/m^3 with a set of pressures varying from 5.83 to 13.58 atm for each feed concentration.

Table 1. Membrane characteristics and geometry (Ion Exchange, India)

Property	Value
Membrane material	TFC Polyamide
Module configuration	Spiral wound
Number of turns	30
Feed spacer thickness (t_f)	0.8 mm
Permeate channel thickness (t_p)	0.5 mm
Module length (L)	0.934 m
Module width (W)	8.4 m
Module diameter	3.25 inches
b *	$8529.45 \left(\frac{\text{atm s}}{\text{m}^4} \right)$
A_w *	$9.5188\text{E-}7 \left(\frac{\text{m}}{\text{atm s}} \right)$
B_s (chlorophenol) *	$8.468\text{E-}8 \left(\frac{\text{m}}{\text{s}} \right)$

* Calculated by Sundaramoorthy et al. [22]

3.2 Model validation

Figs. 1 and 2 depict the comparison of outlet chlorophenol concentration, average permeate concentration, chlorophenol rejection, outlet feed flow, outlet permeate flowrate and outlet feed pressure between the experimental results and the model predictions for three sets of inlet feed flow rate. Generally, the predicted values of the model are in a good agreement with experimental ones over the ranges of pressure and concentration. However, the assumption of constant values of the friction factor, water and solute permeability coefficients for all the experiments had a negative impact on estimating the solute concentrations in both channels. This, in turn leads to reduce the consistency of experimental

and mathematical chlorophenol rejection results ($R^2 = 0.85$). This has provided the prompt to implement a GA platform on the model code for further optimisation as reported in the next section.

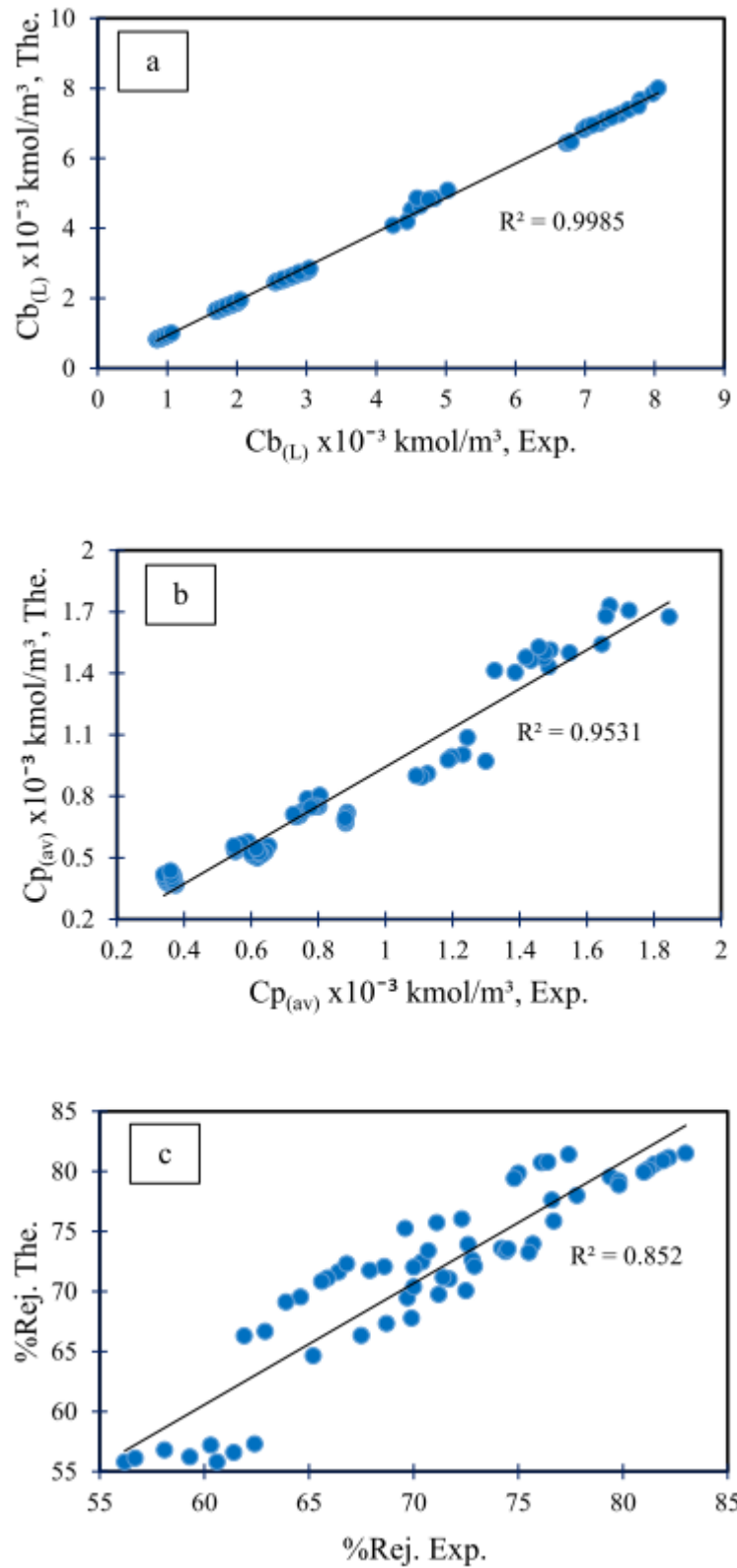


Fig. 1. Experimental and model prediction of (a) outlet feed concentration, (b) average permeate concentration, (c) chlorophenol rejection (inlet conditions mentioned in Section 3)

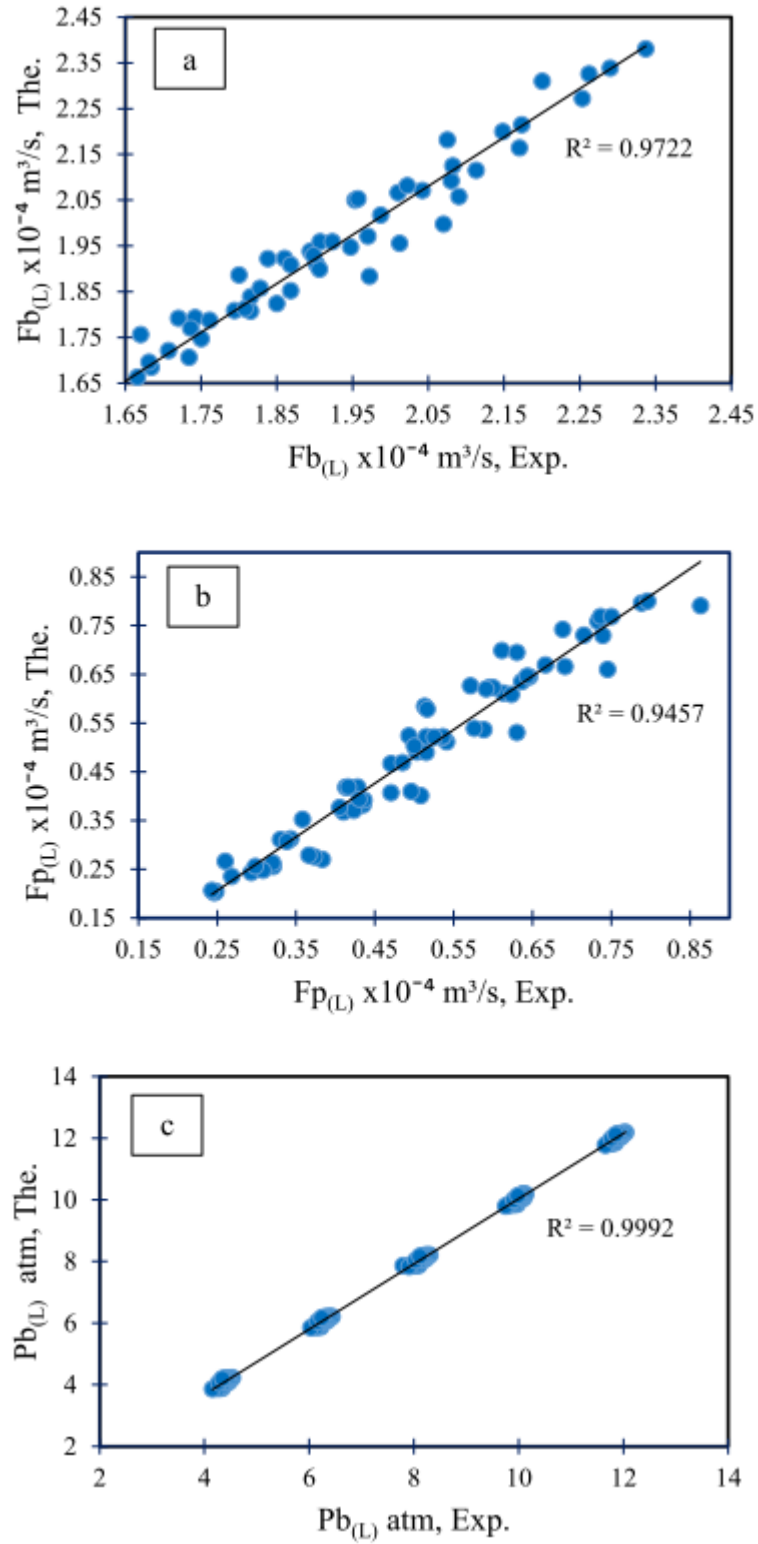


Fig. 2. Experimental and model prediction of (a) outlet feed flow rate, (b) outlet permeate flow rate and (c) outlet feed pressure (inlet conditions mentioned in [Section 3](#))

4. Optimisation of Reverse Osmosis

4.1 Problem description and formulation

The optimisation of the chlorophenol rejection given the lower pressure drop constraint across the membrane with a lower than recommended value is chosen as the objective function for this part of the research. The optimisation technique is based on a GA for the pilot-scale RO wastewater system as used by [Sundaramoorthy et al. \[22\]](#). The experimental data show that the higher achieved rejection of chlorophenol is 83% at inlet concentration ($6.226\text{E-}3 \text{ kmol/m}^3$) with a pressure loss of 1.93 atm. This exceeds the maximum recommended manufacturer value of the selected module. The objective of this optimisation is to find the optimum solute rejection of chlorophenol for each inlet feed concentration (five cases) within the restricted operating conditions of inlet feed flow rate, pressure and temperature. Also, the constraints of 1.38 atm as a maximum overall pressure loss across the membrane length (as declared by the Ion Exchange Ltd. Company, India) has been considered to represent the relative power consumption of each run. The optimisation iteration is individually carried out for five feed concentration of chlorophenol used in the experiments, which varies from $0.778\text{E-}3$ to $6.226\text{E-}3 \text{ kmol/m}^3$. The model transport parameters (A_w , B_s and b) have been considered constant along the optimisation procedure.

The optimisation problem is represented mathematically as follows:

Problem 1:

Max
 $F_{b(0)}, P_{b(0)}, T_b$
Subject to:

Rej

$$P_{loss} \leq P_{loss}^d$$

$$F_{b(0)}^L \leq F_{b(0)} \leq F_{b(0)}^U$$

$$P_{b(0)}^L \leq P_{b(0)} \leq P_{b(0)}^U$$

$$T_b^L \leq T_b \leq T_b^U$$

The model equation and the physical properties are given in [Section 2](#)

The choice of the objective function is to achieve high chlorophenol rejection within the constraints of the decision variables. The limits of the decision variables of the inlet feed flow rate, pressure and temperature and the recommended value of the pressure loss are reported in [Section 5](#).

In line with economic aspects of low energy consumption, [Problem 2](#) is formulated as follows:

[Problem 2:](#)

$$\begin{array}{ll} \text{Max} & Rej \\ F_{b(0)}, P_{b(0)}, T_b & \end{array}$$

$$\begin{array}{ll} \text{Min} & P_{b(0)} \\ F_{b(0)}, P_{b(0)}, T_b & \end{array}$$

Subject to:

$$\begin{aligned} P_{loss} &\leq P_{loss}^d \\ F_{b(0)}^L &\leq F_{b(0)} \leq F_{b(0)}^U \\ P_{b(0)}^L &\leq P_{b(0)} \leq P_{b(0)}^U \\ T_b^L &\leq T_b \leq T_b^U \end{aligned}$$

The model equation and the physical properties are given in [Section 2](#)

The choice of the first objective function is to secure the optimal chlorophenol rejection, while the contribution of the second objective function is to maintain the process of filtration within an accepted consumption of energy (lower operating pressure).

There are two objectives in this problem and the following penalty function is used to balance both objectives and transfer the problem into a single objective optimisation problem as follows:

$$L = W_1 \times Rej - W_2 \times P_{b(0)}$$

(32)

Weight factors W_1 and W_2 are used to balance the contributions of each objective. Then, the original problem will be changed as:

$$\begin{array}{l} \text{Max} \\ F_{b(0)}, P_{b(0)}, T_b \end{array} \quad L$$

Subject to:

$$\begin{aligned} P_{loss} &\leq P_{loss}^d \\ F_{b(0)}^L &\leq F_{b(0)} \leq F_{b(0)}^U \\ P_{b(0)}^L &\leq P_{b(0)} \leq P_{b(0)}^U \\ T_b^L &\leq T_b \leq T_b^U \end{aligned}$$

4.2 Genetic Algorithm

Genetic algorithm (GA) was originally proposed by Holland [6] and is a stochastic and population-based optimisation technique constructed on the perceptions of natural evolution and the biological principles of natural selection. GAs have been successfully applied in various engineering optimisation problems [24] and [25].

The procedure of a GA is shown in Fig. 3. Initially, a population, which consists of a number of individuals, is randomly generated within the lower and upper limits of decision variables.

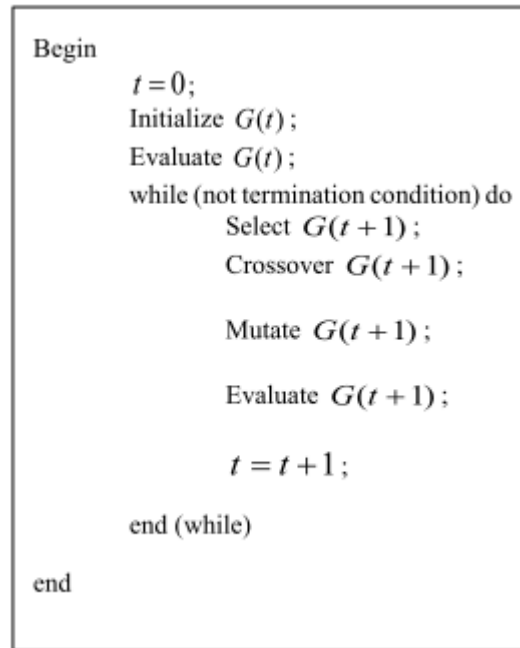


Fig. 3. GA structure.

There are two typical ways of representing individuals in GA context. Traditionally, an individual was represented as a chromosome, i.e. as a bit string. This method took idea of stems from the work of DNA and fits well suitable for integer decision variables. However, more and more researchers prefer a nature representation, i.e. one they are based on float numbers. In this paper, an individual is therefore presented as a vector of real numbers of decision variables.

1. The concept of selection is used to select individuals from the current generations and copy them to formulate a new generation based on their fitness. Usually, an individual with a higher fitness will have a large probability to survive in the next generation. In this paper, a *roulette-wheel method* is used to select individuals from the

current population. Supposing that F_i is the fitness of individuals i , its probability of being selected can be calculated as:

$$P_i = \frac{F_i}{\sum_{j=1}^{N_p} F_j} \quad (33)$$

Where N_p is the population size. An example of the roulette-wheel selection is shown in Fig. 4. A proportion of a wheel is assigned to each individual based on their fitness or selected probability. A random number between $[0,360]$ is generated to determine how many angle the wheel will rotate and the individual pointed by the arrow will be selected and copied to the next generation until N_p individuals have been selected. Fig. 4 also shows that an individual with higher fitness will occur more area and then has higher possibility to be selected.

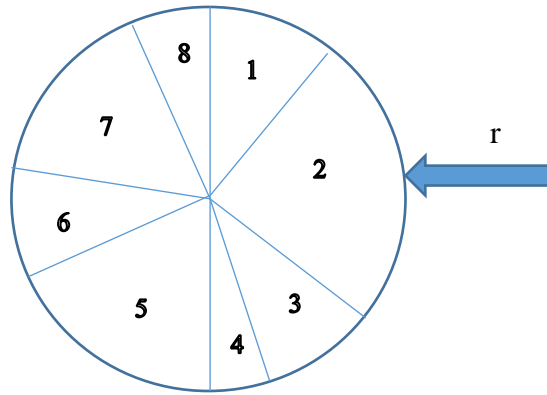


Fig. 4. Roulette-Wheel Selection

2. The concept of crossover is to use to select parents from the new formulated population to generate off springs with a probability of P_c . The crossover method depends on the representation of individuals. For example, if individuals are represented as chromosomes (i.e. a string of bites), the crossover method could be one-point or two-points crossover. In this paper, since individuals are represented as a vector of real

numbers, the crossovers are performed as intermediate recombination, so that the offspring O of a randomly chosen parent S and T is expressed as follows:

$$x_0 = x_T + U(x_S - x_T)$$

(34)

Where U is a uniformly distributed random number over $[0, 1]$.

3. The concept of mutation is used to allow a randomly chosen individual to move to a new position with a probability of P_m . The parent selection method is similar to the one of selecting parents for crossover. Supposing a parent has been selected, a random number, j , between 1 and m (the dimension of decision variables), the corresponding variable will be mutated by using the following uniform mutation will be applied.

$$X'_j = x_j + R(x_j^u - x_j^l)$$

(35)

Where R is a uniformly distributed random number over $[-1, 1]$ and x_j^u, x_j^l are the upper and lower limits respectively of variable j .

Interestingly, one of the most important characteristics of GAs is to generate a number of different solutions for the specified problem at the end of each iteration as opposed to a single solution. This is carried out without requiring good initial guesses for the decision variables [5]. This approach will give a wide area to choose the desired optimised chlorophenol rejection for each input data of operation. GAs are considered to be global optimisation methods, while gradient-based methods can only find a local solution. For the above reasons, the GA technique has been applied to maximize the rejection of wastewater treatment RO system and this is described in more detail in the next section.

5. Numerical Results

5.1 Inlet feed concentration problem

The optimisation study focuses on using genetic algorithms to locate the best operating parameters for the optimum rejection of chlorophenol using a single spiral-wound RO membrane element. The optimisation technique will be implemented in the actual experiments as carried out by [Sundaramoorthy et al. \[22\]](#) using five cases of different inlet feed concentration $0.778\text{E-}3$, $1.556\text{E-}3$, $2.335\text{E-}3$, $3.891\text{E-}3$ and $6.226\text{E-}3$ kmol/m³ with the following operating specification of maximum and minimum inlet feed flow rate, pressure and temperature of $1\text{E-}4 - 1\text{E-}3$ m³/s, $4 - 24.77$ atm and $15 - 40$ °C respectively. Also, this optimisation will be committed with a constraint of an allowable pressure drop (P_{loss}^d) across the membrane length of 1.38 atm. The specified bounds of operating parameters are as recommended by the manufacturer of the membrane.

5.2 Parameter settings

The RO model was coded in Matlab and solved using the modelling and optimisation system¹. The system can readily be implemented using Matlab and Excel to build complex optimisation models. The GA parameters used to explore optimal solutions are given in [Table 2](#).

Table 2. GA Parameters

Parameter	no.
Maximum generation, N_{gen}	500
Population size, N_{pop}	50
Crossover probability, P_c	0.6
Mutation probability, P_m	0.1

¹ <http://www.scholarpark.co.uk/mos> (A modelling and optimisation platform developed by researchers).

5.3 Effects of GA parameters

There are several GA parameters including weight factors, number of generations and crossover and mutation probabilities. This section assesses the performance of GA used to solve different cases of RO optimisation by analysing the effects of parameters used.

The inlet feed concentration of $6.226\text{E-}3 \text{ kmol/m}^3$ in Problem 2 is chosen to analyse the GA performances and to identify the best parameter settings for solving the developed RO optimisation problems.

5.3.1 Effects of weight factor

There are two weight factors W_1 and W_2 as shown in Eq. (45), where W_1 is always set to 1 to simplify the analysis, as the maximum value of Rejection is 1 and the maximum value of Pb_0 is about 25. When, $W_2 = \frac{1}{25} = 0.04$, both objectives are of the same importance. The results of Table 3 show that a value of 0.04 for W_2 offers high chlorophenol rejection with economic operating pressure and allowable temperature. While, any further reduction in W_2 slightly increases the rejection parameter and requires higher operating pressure. Moreover, an increase of W_2 of a value larger than 0.04 has no significant impact, and the output results of optimum rejection and decision variables remain the same. This is because the operating pressure has reached the lower limit. The increase of W_2 cannot increase the contribution of the pressure to the objective function.

Table 3. The influence of the weight factor on GA results

W_2	Rej	Fb_0	Pb_0	Tb
0.001	0.95	2.3698E-4	21.43	40
0.005	0.92	2.0418E-4	11.18	40
0.01	0.90	1.9235E-4	7.57	40
0.04	0.90	1.9224E-4	7.53	40
0.08	0.90	1.9224E-4	7.53	40
0.1	0.90	1.9224E-4	7.53	40
0.2	0.90	1.9224E-4	7.53	40

Where $P_{\text{loss}} = 1.38 \text{ atm}$

5.3.2 Effects of generations

Table 4 shows the influence of using different numbers of generations with a population size of 50 at the optimum weight W_2 of 0.04. As expected, the larger the generation, the easier the GA will identify the solution. This is because there are more chances to explore the space and more fitness evaluations are therefore needed. It is observed that any generation between 80 and 200 can offer an optimum solution for the problem within the recommended decision variables.

This observation can be applied to the effect of population size. The larger the population size, the easier will find a solution and more fitness evaluations are required. Generally, if a small population size is used, a larger generation is required; while when a large population size is applied, a small generation is needed. In this example, the combination of those two parameters is that the population size is 50 and the minimum generation is 80.

Table 4. The influence of the generation number on GA results

Generation	Rej	P _{loss}	Fb ₀	Pb ₀	Tb
10	0.87	0.82	1.2387E-4	7.53	38.1
20	0.89	0.70	1.0700E-4	7.53	40
50	0.90	1.36	1.8933E-4	7.53	40
80	0.90	1.38	1.9224E-4	7.53	40
100	0.90	1.38	1.9224E-4	7.53	40
200	0.90	1.38	1.9224E-4	7.53	40

5.3.3 Effects of crossover probability and mutation probability

Table 5 shows the influence of the crossover probability varied between 0.1 and 0.5 at a mutation probability (P_m) of 0.1 for W_2 of 0.04, 100 generation and a population size of 50 on the output results of GA. It is observed that an increase in the crossover probability has no influence. Furthermore, the impact of mutation probability variation is insignificant as can be shown in Table 6, where it is varied between 0.01 and 0.5 with constant values of crossover

probability of 0.4. Nevertheless, it is affordable to use P_m between 0.01 and 0.02 in order to achieve a lower pressure drop than the other tested values.

Table 5. The influence of the crossover probability on GA results

P_c	Rej	Fb_0	Pb_0	Tb
0.1	0.90	1.9224E-4	7.53	40
0.2	0.90	1.9224E-4	7.53	40
0.3	0.90	1.9224E-4	7.56	40
0.4	0.90	1.9224E-4	7.53	40
0.5	0.90	1.9224E-4	7.53	40

Where $P_{loss} = 1.38$ atm

Table 6. The influence of the mutation probability on GA results

P_m	Rej	P_{loss}	Fb_0	Pb_0	Tb
0.01	0.90	1.37	1.9139E-4	7.53	40
0.02	0.90	1.36	1.8990E-4	7.53	40
0.05	0.90	1.38	1.9221E-4	7.56	40
0.4	0.90	1.38	1.9224E-4	7.53	40
0.5	0.90	1.38	1.9224E-4	7.53	40

The above results of investigating the impact of GA computational parameters show the applicability of obtaining a number of different results, which offers a number of solutions for a specific optimisation problem, especially for the case of altering the weight factor W_2 .

5.3.4 Summaries of effects of parameters

Conclusion, in order to find the global solution of a RO problem, if the population size is set as 50, the minimum generation should be 80. Of course, the larger generation is good for a GA to explore global solutions. Crossover and mutation probability has little influence on the performances for this problem. This means any crossover and mutation probability can be used in those problems.

Weight factors have a big influence on the optimal result. In the above case, if W_1 is set as 1, that $W_2 = 0.04$ means that both objectives are the same important and have the same contribution of the system objective. If chlorophenol rejection is important, W_2 should be a small number, or it should be a larger number.

5.4 Discussion of results

The optimisation problems of one and two objective functions were solved using the proposed GA described in Section 4 and linked with the proposed model of Section 2.

The optimisation results of Problem 1 for each inlet feed concentration and the optimized decision variables obtained are given in Table 7. The GA optimisation results show that a maximum chlorophenol rejection for all five cases can be achieved within operating parameters of inlet feed flow rate, pressure and temperature of $1.046 - 1E-4 \text{ m}^3/\text{s}$, $24.7717 - 16.09 \text{ atm}$ and $15 - 40 \text{ }^\circ\text{C}$ respectively. It can be observed that the removal efficiency of chlorophenol can be increased within the maximum allowable pressure. However, lower values of the operating feed flow rate are required to ensure lower pressure loss along the membrane length, which enhances the flux of water through the membrane and reduces the permeate concentration. Also, the lower feed flow rate can secure the full rejection of chlorophenol from its aqueous solution by maintaining the solution for a longer resident time inside the unit. In contrast to case 1 with higher concentration, the optimisation results of

medium and low concentrations (cases 2 to 5) are within a low feed temperature. One of the key outcomes of this is the optimizer can use such decision variables in cold areas.

At medium and low feed concentration, it appears that there are competitive impacts of pressure, flow rate and temperature, which determine the chlorophenol rejection. The elevating of temperature has two different impacts regarding the rejection parameter of the RO wastewater treatment. The first one is to enhance water flux by decreasing the viscosity parameter and thermal expansion of the membrane [26], and at the same time increasing the organic solute diffusion and absorption through the membrane. This can readily plug the pores of membrane [27] and deteriorates the rejection. However, the combined impact of feed pressure and flow rate has been used in this research to elevate the rejection at lower temperature. Also, for these cases, the Matlab code has been used to test the rejection parameter at higher temperature, and the results show a clear increase in solute flux and a decrease in chlorophenol rejection. From the results of Table 7, the problem appears multimodal problem i.e. with the possibility of more than one solution. This is why for some cases, the temperature is near the upper limits and sometimes, the proposed GA finds a solution, in which the temperature is near the lower limit.

Table 7. Optimal values for Problem 1

Case	Feed conc. $C_{b(0)} \times 10^3$, kmol/m ³	Rej (Max.) Sundaramoorthy et al. [22]	Experimental P_{loss} , Sundaramoorthy et al. [22]	GA Rej	GA P_{loss}	Decision variables		
						$F_{b(0)}$	$P_{b(0)}$	T_b
1	6.226	0.83	1.93	0.98	0.42	1.0464E-4	24.77	40
2	3.891	0.77	1.89	0.99	0.39	1E-4	21.64	15
3	2.335	0.75	1.84	0.99	0.39	1E-4	18.87	15
4	1.556	0.72	1.79	0.99	0.39	1E-4	17.48	15
5	0.778	0.66	1.74	0.99	0.39	1E-4	16.09	15

For a better understanding of the temperature influence at high feed concentration, [case 1](#) is used to analyse the impact of varying the temperatures. Table 8 shows that the chlorophenol rejection has slightly dropped with the decrease of the up limit of temperatures.

Table 8. The up limit of temperature on results for [case 1](#) of [Problem 1](#)

Up limit of Temperature	GA Rej	GA P_{loss}	Decision variables		
			$F_{b(0)}$	$P_{b(0)}$	T_b
40	0.98	0.42	1.0464E-4	24.77	40
39	0.97	0.43	1.0597E-4	24.77	39
38	0.96	0.45	1.0749E-4	24.77	38
37	0.94	0.46	1.0925E-4	24.77	37
36	0.95	0.41	1E-4	24.77	15
35	0.95	0.41	1E-4	24.77	15
34	0.95	0.41	1E-4	24.77	15

The optimisation results of the [Problem 2](#) for each inlet feed concentration and the optimized decision variables obtained are given in [Table 9](#). The GA optimisation results show that a maximum chlorophenol rejection for all five cases can be achieved within the operating parameters of inlet feed flow rate, pressure and temperature of $1.922 - 1.945E-4 \text{ m}^3/\text{s}$, $7.32 - 7.53 \text{ atm}$ and $40 \text{ }^\circ\text{C}$ respectively. This is comparable to the optimisation results of [Problem 1](#). Here, GA optimisation increases the chlorophenol rejection of five cases by 8.54 , 15.25 , 16.2 , 19.59 , 26.57% respectively, at the same time keeping an allowable pressure drop constraint. It also appears that considering the pressure drop as a constraint actually deviates the optimisation process to raise the rejection parameter by using a lower feed flow rate but at a higher temperature. [Table 9](#) shows that for each case, the temperature has achieved its up limits and the pressure has moved to the lower limits in order to achieve the two objective functions of the problem. This is considered as a positive result when considering comparative results of raising the operating pressure – a well-known key parameter of raising rejection.

Table 9. Optimal values for [Problem 2](#)

Case	Feed conc. $C_{b(0)} \times 10^3$,	Rej (Max.)	Experimental P_{loss} ,	GA	Decision variables
------	-------------------------------------	------------	---------------------------	----	--------------------

	kmol/m ³	Sundaramoorthy et al. [22]	Sundaramoorthy et al. [22]	Rej	Fb ₍₀₎	Pb ₍₀₎	T _b
1	6.226	0.83	1.93	0.90	1.92243E-4	7.53	40
2	3.891	0.77	1.89	0.89	1.93143E-4	7.47	40
3	2.335	0.75	1.84	0.88	1.93936E-4	7.45	40
4	1.556	0.72	1.79	0.87	1.94295E-4	7.41	40
5	0.778	0.66	1.74	0.84	1.94572E-4	7.32	40

Where GA P_{loss} = 1.38 atm

The temperature influence is given in Table 10 for high feed concentration (Case 1). Interestingly, Table 10 shows that the chlorophenol rejection drops with the decrease of the up limit of temperatures. This is due to choosing a minimum operating pressure as an objective function. This might cancelled its impact and results in a reduction in a rejection parameter due to decrease in temperature. This should be compared to using a higher operating pressure as the case of Table 8, which slightly affects the rejection parameter.

Table 10. The up limit of temperature on results for case 1 of Problem 2

Up limit of Temperature	GA Rej	Decision variables		
		Fb ₍₀₎	Pb ₍₀₎	T _b
40	0.90	1.9224E-4	7.53	40
39	0.89	1.9199E-4	7.53	39
38	0.88	1.9172E-4	7.53	38
37	0.87	1.9142E-4	7.53	37
36	0.86	1.9110E-4	7.53	36
35	0.84	1.9076E-4	7.53	35
34	0.83	1.9039E-4	7.53	34

Where GA P_{loss} = 1.38 atm

6. Conclusions

In this study, optimisation of chlorophenol rejection from wastewater is considered using model based techniques. A one-dimensional mathematical model for the prediction of the performance of wastewater spiral-wound RO process is developed and implemented. The

consistency of the proposed model is tested against actual experimental data of chlorophenol rejection from the literature using a pilot-scale RO system with a single spiral-wound membrane element. The model is then augmented with a novel genetic algorithm platform involving two objective functions of maximizing chlorophenol rejection and minimizing the operating pressure for a set of five different feed concentration while maintaining the treatment operation within an allowable pressure loss i.e. with significant energy savings. The results show that the rejection parameter of chlorophenol can be optimized up to 26.57% for the set of five inlet feed concentration and all within the allowable constraint of pressure drop. The results clearly show that RO problems are very complex and multimodal with the net inference that many global solutions may exist. Such other global solutions will be explored in further related research.

References

1. M.G. Marcovecchio, P.A. Aguirre, N.J. Scenna, Global optimal design of reverse osmosis networks for seawater desalination: modeling and algorithm, *Desalination* 184 (2005) 259-271.
2. A. Villafafila, I.M. Mujtaba, Fresh water by reverse osmosis based desalination: simulation and optimisation, *Desalination* 155 (2003) 1-13.
3. Y-y. Lu, Y-d. Hu, D-m. Xu, L-y. Wu, Optimum design of reverse osmosis seawater desalination system considering membrane cleaning and replacing, *Journal of Membrane Science* 282 (2006) 7-13.
4. Z.V.P. Murthy, J.C. Vengal, Optimization of a Reverse Osmosis System Using Genetic Algorithm, *Separation Science and Technology* 41 (2006) 647-663.
5. C. Guria, P.K. Bhattacharya, S.K.Gupta, Multi-objective optimization of reverse osmosis desalination units using different adaptations of the non-dominated sorting

- genetic algorithm (NSGA), *Computers and Chemical Engineering* 29 (2005) 1977-1995.
6. J.H. Holland *Adaptation in natural and artificial systems*. Ann Arbor, MI: University of Michigan Press.; 1975.
 7. E.S. Fraga, T.R. Senos Matias, Synthesis and optimization of a nonideal distillation system using a parallel genetic algorithm, *Computers and Chemical Engineering* 20 (1996) S79-S84.
 8. R. Raj Gupta, S.K. Gupta, Multiobjective optimization of an industrial nylon-6 semibatch reactor system using genetic algorithm, *Journal of Applied Polymer Science* 73 (1999) 729-739.
 9. I.R.S. Victorino, J.P. Maia, E.R. Morais, M.R. Wolf Maciel, R.M. Filho, Optimization for large scale process based on evolutionary algorithms, *Genetic algorithms, Chemical Engineering Journal* 132 (2007) 1-8.
 10. J. Na, K.S. Kshetrimayum, U. Lee, C. Han, Multi-objective optimization of microchannel reactor for Fischer-Tropsch synthesis using computational fluid dynamics and genetic algorithm, *Chemical Engineering Journal* (In-Press)
 11. J.K. Rajesh, S.K. Gupta, G.P. Rangaiyah, A.K. Ray, Multiobjective Optimization of Steam Reformer Performance Using Genetic Algorithm, *Industrial and Engineering Chemistry Research* 39 (2000) 706-717.
 12. F. Fang, B-J. Ni, W-M. Xie, G-P. Sheng, S-G. Liu, Z-H. Tong, H-Q. Yu, An integrated dynamic model for simulating a full-scale municipal wastewater treatment plant under fluctuating conditions, *Chemical Engineering Journal* 160 (2010) 522-529.
 13. B. Djebedjian, H. Gad, I. Khaled, M.A. Rayan, Optimization of reverse osmosis desalination system using genetic algorithms technique, In *Twelfth International Water Technology Conference, IWTC12, Alexandria, Egypt 2008*
 14. T-M. Lee, H. Oh, Y-K. Choung, S. Oh, M. Jeon, J.H. Kim, S.H. Nam, S. Lee, Prediction of membrane fouling in the pilot-scale microfiltration system using genetic programming, *Desalination* 247 (2009) 285-294.
 15. S-M. Park, J. Han, S. Lee, J. Sohn, Y-M. Kim, J-S. Choi, S. Kim, Analysis of reverse osmosis system performance using a genetic programming technique, *Desalination and Water Treatment* 43 (2012) 281-290.

16. K. Bourouni, T. Ben M'Barek, A. Al Taei, Design and optimization of desalination reverse osmosis plants driven by renewable energies using genetic algorithms, *Renewable Energy* 36 (2011) 936-950.
17. C.C. Yuen, Aatmeeyata, S.K. Gupta, A.K. Ray, Multi-objective optimization of membrane separation modules using genetic algorithm, *Journal of Membrane Science* 176 (2000) 177-196.
18. A. Okhovat, S.M. Mousavi, Modeling of arsenic, chromium and cadmium removal by nanofiltration process using genetic programming, *Applied Soft Computing* 12 (2012) 793-799.
19. R. Soleimani, N.A. Shoushtari, B. Mirza, A. Salahi, Experimental investigation, modeling and optimization of membrane separation using artificial neural network and multi-objective optimization using genetic algorithm, *Chemical Engineering Research and Design* 91 (2013) 883-903.
20. H.K. Lonsdale, U. Merten, R.L. Riley, Transport properties of cellulose acetate osmotic membranes, *Journal of Applied Polymer Science* 9 (1965) 1341-1362.
21. M.A. Al-Obaidi, C. Kara-Zaitri, I.M. Mujtaba, Development of a mathematical model for apple juice compounds rejection in a spiral-wound reverse osmosis process, *Journal of Food Engineering* 192 (2017) 111-121.
22. S. Sundaramoorthy, G. Srinivasan, D.V.R. Murthy, An analytical model for spiral wound reverse osmosis membrane modules: Part II — Experimental validation, *Desalination* 277 (2011) 257-264.
23. C. Koroneos, A. Dompros, G. Roumbas, Renewable energy driven desalination systems modelling, *Journal of Cleaner Production* 15 (2007) 449-464.
24. R. Leardi, Genetic algorithms in chemometrics and chemistry: a review, *Journal of Chemometrics* 15 (2001) 559-569.
25. M. Kumar, M. Husian, N. Upreti, D. Gupta, Genetic algorithm: Review and application, *International Journal of Information Technology and Knowledge Management* 2 (2010) 451-454.
26. K. Thirugnanasambandham, V. Sivakumar, K. Loganathan, R. Jayakumar, K. Shine, Pilot scale evaluation of feasibility of reuse of wine industry wastewater using reverse osmosis system: modeling and optimization, *Desalination and Water Treatment* 57 (2016) 25358-25368.

27. Y. Li, J. Wei, C. Wang, W. Wang, Comparison of phenol removal in synthetic wastewater by NF or RO membranes, *Desalination and Water Treatment* 22 (2010) 211-219.

Appendix A

The diffusivity of brine and permeate $D_{b(x)}$ and $D_{p(x)}$ (m^2/s) are given by the relations.

$$D_{b(x)} = 6.725E - 6 \exp \left\{ 0.1546E - 3 C_{b(x)} \times 18.01253 - \frac{2513}{T_{b(x)} + 273.15} \right\}$$

(1)

$$D_{p(x)} = 6.725E - 6 \exp \left\{ 0.1546E - 3 C_{p(av)} \times 18.01253 - \frac{2513}{T_{p(x)} + 273.15} \right\}$$

(2)

While the viscosity of brine and permeate $\mu_{b(x)}$ and $\mu_{p(x)}$ ($kg/m s$) are given by the relations.

$$\mu_{b(x)} = 1.234E - 6 \exp \left\{ 0.0212E - 3 C_{b(x)} \times 18.0153 + \frac{1965}{T_{b(x)} + 273.15} \right\} \quad (3)$$

$$\mu_{p(x)} = 1.234E - 6 \exp \left\{ 0.0212E - 3 C_{p(av)} \times 18.0153 + \frac{1965}{T_{p(x)} + 273.15} \right\} \quad (4)$$

The density of brine and permeate $\rho_{b(x)}$ and $\rho_{p(x)}$ (kg/m^3) are given by the equations below:

$$\rho_{b(x)} = 498.4 m_{f(x)} + \sqrt{[248400 m_{f(x)}^2 + 752.4 m_{f(x)} C_{b(x)} \times 18.0153]} \quad (5)$$

$$\rho_{p(x)} = 498.4 m_{p(x)} + \sqrt{[248400 m_{p(x)}^2 + 752.4 m_{p(x)} C_{p(av)} \times 18.0153]} \quad (6)$$

Where:

$$m_{f(x)} = 1.0069 - 2.757E - 4 T_{b(x)}$$

(7)

$$m_{p(x)} = 1.0069 - 2.757E - 4 T_{p(x)}$$

(8)

The Reynolds number along the feed and permeate channels

$Re_{b(x)}$ and $Re_{p(x)}$ (dimensionless) can be calculated from:

$$Re_{b(x)} = \frac{\rho_{b(x)} de_b F_{b(x)}}{t_f W \mu_{b(x)}} \quad (9)$$

$$Re_{p(x)} = \frac{\rho_{p(x)} de_p J_w(x)}{\mu_{p(x)}}$$

(10)

Where de_b and de_p (m) are the equivalent diameters of the feed and permeate channels respectively.

$$de_b = 2t_f \quad (11)$$

$$de_p = 2t_p$$

(12)

t_f and t_p (m) are the heights of feed and permeate channels.

